CONF-9409342--5
LBL-36370
UC-414

Lawrence Berkeley Laboratory
UNIVERSITY OF CALIFORNIA

Presented at the International Workshop on Multiparticle Correlations and Nuclear Reactions, Nantes, France, September 5–9, 1994, and to be published in the Proceedings

The Dynamics of Fragment Formation

D. Keane and The EOS Collaboration

September 1994

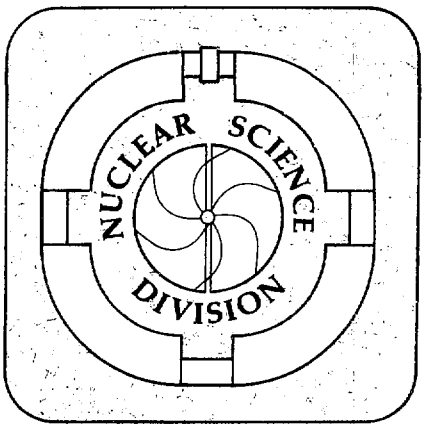

Prepared for the U.S. Department of Energy under Contract Number DE-AC03-76SF00098

LBL-36370
UC-414

Presented at the International Workshop on Multiparticle Correlations
and Nuclear Reactions, Nantes, France, 5-9 Sept. 1994,
and to be published in the Proceedings

The Dynamics of Fragment Formation

D. Keane
Kent State University
Kent, OH 44242

and

The EOS Collaboration

September 1994

This work was supported by the Director, Office of Energy Research, Division of Nuclear Physics of the Office of High Energy and Nuclear Physics of the U.S. Department of Energy under Contracts DE-AC03-76SF00098, DE-FG02-89ER40531, DE-FG02-88ER40408, DE-FG02-88ER40412, DE-FG05-99ER40437 and by the National Science Foundation under Grant PHY-9123301.

THE DYNAMICS OF FRAGMENT FORMATION

D. KEANE,[2] J. AICHELIN,[7] S. ALBERGO,[6] F. BIESER,[1] F. P. BRADY,[4]
Z. CACCIA,[6] D. A. CEBRA,[4] A. D. CHACON,[5] J. L. CHANCE,[4]
Y. CHOI,[3] * S. COSTA,[6] J. B. ELLIOTT,[3] M. L. GILKES,[3] †
P.-B. GOSSIAUX,[7] J. A. HAUGER,[3] A. S. HIRSCH,[3] E. L. HJORT,[3]
A. INSOLIA,[6] M. JUSTICE,[2] J. KINTNER,[4] M. A. LISA,[1] H. S. MATIS,[1]
M. MCMAHAN,[1] C. MCPARLAND,[1] D. L. OLSON,[1] M. D. PARTLAN,[4]
N. T. PORILE,[3] R. POTENZA,[6] G. RAI,[1] J. RASMUSSEN,[1]
H.-G. RITTER,[1] J. ROMANSKI,[6] J. L. ROMERO,[4] G. V. RUSSO,[6]
R. P. SCHARENBERG,[3] A. SCOTT,[2] Y. SHAO,[2] ‡ B. K. SRIVASTAVA,[3]
T. J. M. SYMONS,[1] M. L. TINCKNELL,[3] C. TUVÈ,[6] S. WANG,[2]
P. G. WARREN,[3] D. WEERASUNDARA,[2] H. H. WIEMAN,[1] and
K. L. WOLF[5]

[1] *Lawrence Berkeley Laboratory, University of California, Berkeley, CA 94720*
[2] *Kent State University, Kent, Ohio 44242*
[3] *Purdue University, West Lafayette, Indiana 47907*
[4] *University of California, Davis, California 95616*
[5] *Texas A&M University, College Station, Texas 77843*
[6] *Università di Catania and INFN-Sezione di Catania, 95129 Catania, Italy*
[7] *Université de Nantes, F-44072 Nantes Cedex 03, France*

ABSTRACT

We demonstrate that in the Quantum Molecular Dynamics model, dynamical correlations can result in the production rate for final state nucleon clusters (and hence composite fragments) being higher than would be expected if statistics and the available phase space were dominant in determining composite formation. An intranuclear cascade or a Boltzmann-Uehling-Uhlenbeck model, combined with a statistical approach in the late stage of the collision to determine composites, provides an equivalent description only under limited conditions of centrality and beam energy. We use data on participant fragment production in Au + Au collisions in the Bevalac's EOS time projection chamber to map out the parameter space where statistical clustering provides a good description. In particular, we investigate momentum-space densities of fragments up to ^{4}He as a function of fragment transverse momentum, azimuth relative to the reaction plane, rapidity, multiplicity and beam energy.

*Current address: Sung Kwun Kwan University, Suwon 440-746, Republic of Korea.
†Current address: State University of New York, Stony Brook, NY 11794.
‡Current address: Crump Institute for Biological Imaging, Univ. of California, Los Angeles, CA 91776.

1. Introduction

One of the first results to emerge after heavy-ion experiments at several hundred MeV per nucleon became possible in the mid-1970s was the observation that there is a simple relationship between the spectra of protons and composite fragments: the observed invariant momentum-space density ρ_A for fragments with mass number A and momentum $A\mathbf{p}$ closely follows the Ath power of the observed proton density ρ_1^A at momentum $\mathbf{p}$.[1–3] This power law behavior was found to hold for momentum spectra of fragments up to $A = 4$ with projectiles ranging from ^{12}C to ^{139}La at a variety of beam energies between $0.25A$ GeV and $2.1A$ GeV; some deviations occur for spectra at small laboratory polar angles where fragment emission from the projectile spectator becomes important. Fragments up to $A = 14$ emitted at large polar angles in collisions of Ar ions near $100A$ MeV were also found to follow the momentum-space power law.[4] More recently, the power law has been observed to hold in collisions of projectiles ranging from protons to Au at the maximum energy of the Brookhaven AGS.[5,6] These observations are consistent with a simple picture in which the concept of a cluster of nucleons has no meaning during the early, high-density stages of the collision; as the system expands and the rate of hard nucleon-nucleon scattering decreases, nucleons which by chance lie close to each other in position and velocity can coalesce. In the picture suggested by the experimental data, clusters undergo sufficient cycles of coalescence and breakup during the late stage of the collision for chemical equilibrium to be approached or reached by the time all nucleon-nucleon scattering ceases.

While the momentum-space power law suggests a simple statistical mechanism of fragment formation late in the collision time-evolution, there are contrasting indications from nuclear transport models that dynamical correlations can strongly influence the final-state configuration of nucleon clusters and these correlations originate surprisingly early.[7–9] How can such indications be reconciled with the fact that models assuming thermal equilibrium provide reasonable descriptions of the collision process? Recent experiments which point to about half the available energy being associated with collective undirected expansion[10–13] may help in this reconciliation. In the present work, we begin by studying Au + Au events generated by the Quantum Molecular Dynamics (QMD) model[7] in order to probe the conditions of bombarding energy and centrality where QMD indicates that dynamical correlations are important for fragment production. Then we proceed to investigate fragment production in Au + Au collisions in the Bevalac's EOS time projection chamber.

2. Dynamical Correlations and Fragment Production in QMD

In the Quantum Molecular Dynamics model,[7,8] the time-evolution of the full multi-nucleon phase space distribution is followed. Nucleons are represented by Gaussian wave packets which move under the influence of mutual density-dependent two-

body interactions and collisions. This model preserves all correlations which are present initially or are built up in the course of the reaction. It replaces the mean fields of one-body transport models, such as those based on the BUU/VUU approach,[14] by true two-body interactions. Consequently, QMD is uniquely suited for studies involving the interplay between cluster formation and collision dynamics at the nucleon level. At times on the order of 200 fm/c after the start of the interaction, the nucleon clusters are well separated from each other in coordinate space, and the fragments can readily be determined through a minimum spanning tree procedure. It is assumed that a nucleon within a distance 3 fm$< r_{min} <$5 fm from another nucleon is a member of the same cluster. These limits are determined by the average separation of two nucleons in nuclear matter and by the range of the interaction; the exact value makes no significant difference in the context of the present investigation.

We simulate Au on Au reactions at 60A MeV and 600A MeV, using QMD with a soft momentum-dependent equation of state.[7] Our method for testing the importance of dynamical correlations in fragment production involves the event mixing technique. Mixed QMD events are generated by randomly choosing each nucleon from a different real QMD event, and these nucleons are selected under the constraint that the single-particle-inclusive spectra for each impact parameter are the same. In this application, we preserve the orientation of the nucleons with respect to the event reaction plane in the mixed events. Thus, mixed QMD events can no longer contain the dynamical correlations relevant to fragment production, and these events can be considered equivalent to the output of a BUU model.

In a situation where fragments are predominantly determined by statistics and the one-body phase space density, a BUU or intranuclear cascade model should provide an adequate description if a switch is made to a coalescence or other clustering prescription at an appropriate stage of the time-evolution. Normally, hybrid models of this type make the switch at a much earlier time than the $\sim$ 200 fm/c when the QMD calculation is stopped. In order to construct a conventional hybrid model using our mixed QMD events, we should either trace back the nucleons to an earlier time, or equivalently, we should use the standard QMD clustering algorithm with a larger value of r_{min}. We choose the latter approach, and we search for a single r_{min} that yields the same abundances of deuterons, αs and intermediate mass ($4 < A < 32$) fragments as the original QMD calculation; if such an r_{min} does not exist, we interpret this as evidence for dynamical correlations playing a significant role in fragment formation. For 60A MeV Au + Au, no single r_{min} exists that even remotely satisfies this criterion at any impact parameter. For all possible r_{min} in the hybrid calculation, α particle yields remain a factor of about 3 below QMD, and IMF yields remain an order of magnitude below QMD (for further details, see ref.[9]). Thus we conclude that dynamical correlations cannot be neglected in a heavy system at 60A MeV. In contrast, we find that r_{min} = 9 fm does meet the yield-matching criterion in the case of central 600A MeV Au + Au collisions, and $r_{min} \sim$ 10 fm comes close for non-central collisions. Note, however, that satisfying the r_{min} criterion is a necessary but insufficient condition for dynamical correlations to be destroyed during the high

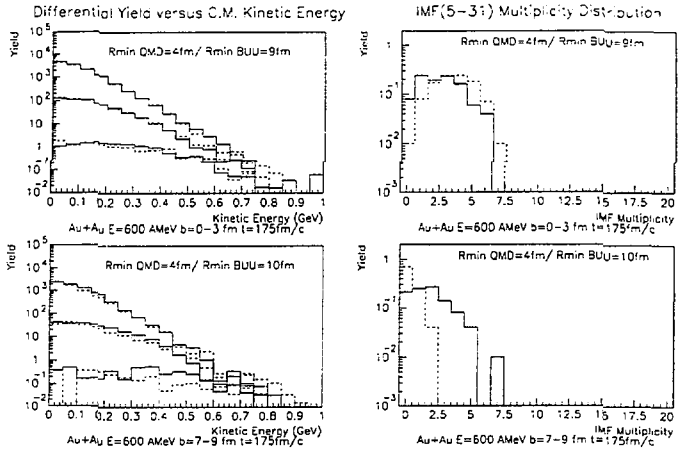

Figure 1: Kinetic energy distributions for $A = 1$, 2 and 4 (left) and IMF multiplicities (right) from 600A MeV Au + Au for QMD (full line) with $r_{\min} = 4$ fm and for the hybrid model (dashed line) with optimal $r_{\min}$, namely 9 fm for central collisions (top) and 10 fm for non-central collisions (bottom).

density phase of the collision.

A more comprehensive test of the convergence between QMD and our hybrid simulation based on mixed QMD events is provided by energy spectra for various fragment species and by multiplicity spectra. The upper left panel of Fig. 1 presents c.m. energy spectra for protons, deuterons and αs (whose yields decrease in that order) for central (0 to 3 fm) 600A MeV Au + Au collisions; the solid-line histograms are for QMD and the dashed histograms are for the hybrid simulation with $r_{\min} = 9$ fm. The lower left panel presents the same comparison for more peripheral collisions (7 to 9 fm) and with $r_{\min} = 10$ fm in the hybrid simulation. Similarly, the two panels on the right of Fig. 1 compare intermediate-mass fragment (IMF) multiplicity spectra for central and non-central collisions. It can be seen that the hybrid BUU-like approach adheres consistently to the QMD calculation for central collisions. In the case of the larger impact parameters, agreement among light fragments is a little worse but still acceptable, while IMF multiplicities are substantially underpredicted by the hybrid calculation.

Overall, we are led to the conclusion that for less violent collisions, the system preserves some memory of its individual initial-state configuration; the final state nu-

cleons can be strongly correlated and the system can remain far from an equilibrated state. In more violent collisions (e.g., central Au + Au at 600A MeV) the number of hard scattering interactions is much larger, in part due to less Pauli blocking, and the system comes closer to exploring the full available phase space. Only then does the approximation of a decorrelated system become appropriate when considering fragment production. In this preliminary investigation, we do not directly compare the QMD model to experiment, but we use the findings of this section as motivation for a new study of statistical coalescence among charged-particle-exclusive measurements for a heavy system.

3. Observed Fragment Production in Au + Au Collisions

3.1 The EOS Detector and Event Selection

In this investigation, we use data from the EOS time projection chamber (TPC), which was in operation at Lawrence Berkeley Laboratory's Bevalac during 1992. This TPC is the principal subsystem of the EOS detector; it has rectangular geometry and operated in a 1.3 T magnetic field. Details about the detector and its performance can be found elsewhere.[15-17] We report results for fragments emitted forward of mid-rapidity, where acceptance is optimum; our samples after multiplicity selection contain about 35,000 events at a beam energy of 1.15A GeV, and typically, 6,000 events each at 1.0A, 0.8A, 0.6A and 0.25A GeV. Following the convention introduced by the Plastic Ball group, we characterize the centrality of collisions in terms of baryonic fragment multiplicity M as a fraction of $M_{\rm max}$, where $M_{\rm max}$ is a value near the upper limit of the M spectrum where the height of the distribution has fallen to half its plateau value.[18] Mult 1 through Mult 4 denote the four intervals of M with upper boundaries at 0.25, 0.5, 0.75 and 1.0 times $M_{\rm max}$, respectively, and Mult 5 denotes $M > M_{\rm max}$.

3.2 Momentum-Space Power Law Behavior at 1.15A GeV

To assess the extent to which a coalescence prescription describes light composite fragment production in the EOS TPC, we first use our largest sample (1.15A GeV Au + Au) to test the agreement between the shapes of $\rho_A(x)$ and $\rho_1^A(x)$, where x is any observable such that ρ varies significantly over its range. The solid circles in the upper panels of Fig. 2 show the dependence on $p^\perp/A$ of the deuteron density $\rho_2 = kA^2 dN/p^\perp dp^\perp$ for Mult 4 events in five intervals of center-of-mass rapidity y', where y' denotes rapidity divided by the projectile rapidity. The constant k is a normalization factor, and the ordinate has arbitrary units. We show the relative proton density as solid curves normalized to the same area, and the normalized proton density squared is given by the dashed curves. This normalization is equivalent to

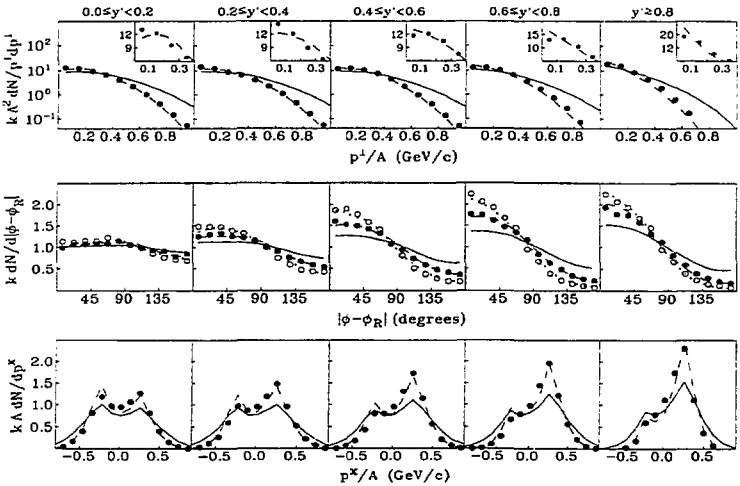

Figure 2: Relative momentum-space density for deuterons (solid circles), protons (solid curves) and relative proton density squared (dashed curves) in Mult 4 collisions of 1.15A GeV Au + Au as a function of transverse momentum per nucleon (top), azimuth relative to the event reaction plane (center), and transverse momentum per nucleon projected on the reaction plane (bottom). In the center panels, the open circles indicate the density for fragments with $A = 3$ and the dotted curves the density for deuterons to the power of 3/2.

optimizing coalescence coefficients $C_A = \rho_A/\rho_1^A$ separately in each y' interval. In fact we find that the optimized C is flat within errors over participant rapidities, up to $y' \sim 0.7$ or 0.8; further details are reported elsewhere.[19] Statistical uncertainties approach the symbol size near the upper end of the $p^\perp/A$ scale, but are far smaller at the lower end. Accordingly, the insets in the upper right corners show the same data with better resolution at lower $p^\perp/A$, using a linear scale on the ordinate. These results for high multiplicity Au + Au collisions show a level of adherence to power law behavior that is comparable to what was reported previously for single-particle-inclusive measurements, and demonstrate the persistence of momentum-space coalescence behavior for a larger mean number of participant nucleons.

We do not expect to observe power law behavior in regions where the assumptions underlying the simple momentum-space coalescence model do not hold, for example, where proton and neutron spectra differ due to Coulomb effects. For all results that follow, a cut requiring $p^\perp/A \geq 0.2$ GeV/c is imposed, except in the determination of **Q**, described below, or where explicitly noted.

The center panels of Fig. 2 show the dependence of phase-space density on $|\phi - \phi_R|$, the azimuthal angle of fragment i relative to the event reaction plane as defined by the vector $\mathbf{Q}_i = \sum_{j \neq i}^{M} w(y'_j)\mathbf{p}_j^{\perp}$.[20] The weighting factor $w(y'_j)$ is designed to optimize the correlation of $\mathbf{Q}$ with the reaction plane; we follow the prescription $w(y'_j) = \min(1,\ y'_j/0.8)$, where $y' > 0$. Here, the normalization factor k is chosen so that the mean ordinate is 1. The solid circles, the solid curves and the dashed curves have the same meaning as in the upper panels, while the open circles denote the relative density of fragments with $A = 3$ and the dotted curves denote the three-halves power of the deuteron density. We choose to plot $\rho_2^{3/2}$ in place of ρ_1^3; these two quantities are close to each other, but ρ_1^3 can have a larger uncertainty because of the larger exponent. There is a considerable body of experimental literature[21-26] describing an increase with A of observables related to the mean in-plane transverse momentum per nucleon $\langle p^x(y)/A \rangle$.[20] This phenomenon was first suggested by hydrodynamic models,[27] in which collective effects were seen more clearly for heavier fragments. Quantum Molecular Dynamics also exhibits a mass dependence, attributed to early formation and sideward deflection of light and intermediate-mass composites.[8] The mass dependence of $\langle p^x(y)/A \rangle$ persists when the standard $p^{\perp}$ cut is applied to our data. The lower panels of Fig. 2 show relative p^x/A densities for protons and deuterons using the same symbols as before. The combination of power law behavior and the asymmetry in the p^x distribution can suffice to explain the A dependence of $\langle p^x(y)/A \rangle$ for $p^{\perp}/A \geq 0.2$ GeV/c.

In Fig. 3, we investigate p^x/A densities for 1.15A GeV Au + Au (Mult 4) in more detail. The upper row of panels displays the same spectra as in the lower panels of Fig. 2, namely deuteron density (circles), proton density (solid curve) and proton density squared (dashed curve), except that the usual condition $p^{\perp}/A \geq 0.2$ GeV/c has not been applied. The middle row of panels shows α particle density as triangles, deuteron density as a solid line, and deuteron density squared as a dotted curve, again without the usual $p^{\perp}$ cut. The lower row shows the same quantities as the middle row, but with the condition $p^{\perp}/A \geq 0.2$ GeV/c reimposed. It is evident that without the $p^{\perp}$ cut, momentum-space power law behavior is markedly degraded for α particles, and less seriously degraded for deuterons. In general, in cases where excluding fragments with low $p^{\perp}/A$ improves agreement by a large amount compared with statistical errors, we observe that a softer cut $p^{\perp}/A \geq 0.15$ GeV/c tends to be marginally worse than the standard 0.2 GeV/c cut.

3.3 Azimuthal Densities as Functions of Beam Energy, Rapidity and Centrality

Our $dN/d(\phi - \phi_R)$ spectra, as illustrated in the center panels of Fig. 2, have been fitted to functions of the form $1 + \lambda \cos(\phi - \phi_R) + \alpha \cos 2(\phi - \phi_R)$. The second term allows better fits to be obtained for the strongest azimuthal asymmetries, where there are deviations from a cosine shape. The notation λ_A signifies fit values for fragments with mass A, while $\lambda_{AA'}$ signifies fits to the spectrum for mass A' raised to the power

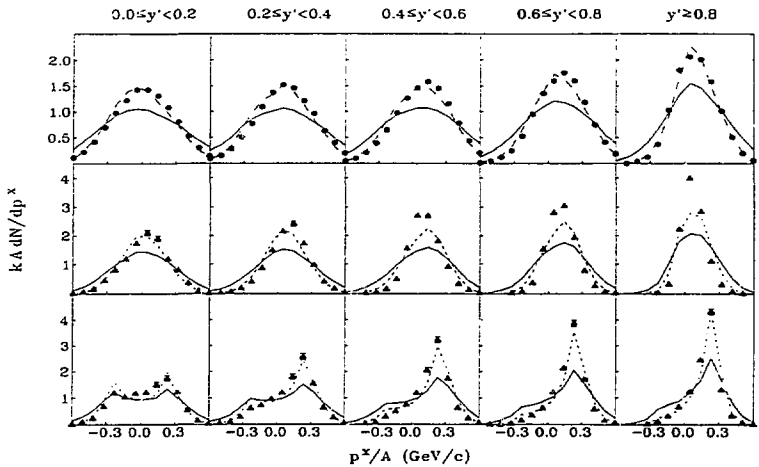

Figure 3: Data for Mult 4 collisions of 1.15A GeV Au + Au, showing relative p^x/A density for deuterons (circles) and α particles (triangles); the dashed curves are proton density squared and the dotted curve are deuteron density squared. The usual condition $p^\perp/A \geq 0.2$ GeV/c has been applied to the lower row of panels only.

of A/A'. In Fig. 4, we present tests of power law behavior through λ comparisons for the full Au + Au sample spanning beam energies between 0.25A GeV and 1.15A GeV. Overall, we conclude that the power law is remarkably consistent in describing fragment flow for $p^\perp/A \geq 0.2$ GeV/c, as parametrized by λ. The most prominent deviation is a tendency for the Ath power of the proton spectra (the open triangles) to overpredict the observed λ values at forward rapidities. The same tendency is not repeated in the deuteron spectra to the power of $A/2$. This deviation has a pattern of dependence on rapidity and multiplicity that is qualitatively consistent with the excess protons having evaporated from the projectile spectator, which is known to experience a sideward deflection in the reaction plane.[18]

An important advantage of the EOS TPC is its good particle identification[16] and its seamless acceptance, which are simple enough to be simulated accurately. Using various event generators, we have compared the observables under investigation before and after filtering through a detailed GEANT-based simulation of the TPC. We find that detector distortions are comparable to or smaller than the symbol sizes

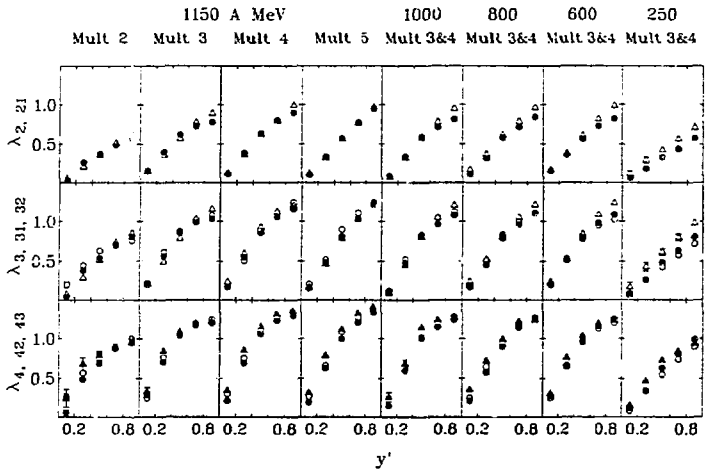

Figure 4: Sideward flow parameters λ as a function of rapidity. The open triangles indicate λ_{A1}, the parameter based on the Ath power of the proton spectrum. The solid circles indicate both λ_2, the parameter for deuterons, and λ_{A2}, the parameter for the deuteron spectrum to the power of $A/2$. Likewise, the open circles indicate λ_3 and λ_{A3}, and the solid triangles indicate λ_4.

or statistical error bars in Figs. 2, 3 and 4.

3.4 Conclusions

A comprehensive study of dynamical correlations as reflected in light and intermediate mass fragment formation in intermediate-energy collisions is a challenging undertaking. While the QMD model implementation used in this work is appropriate for describing the initial phase of the collision and the initial formation of clusters, the slower and much less energetic processes involved in deexcitation of these clusters remains a source of uncertainty when making direct quantitative comparisons of fragment yields with experiment. In these proceedings, we focus on the relatively modest objective of identifying conditions where dynamical correlations can be neglected and where simple statistical processes determine fragment production. QMD suggests

that these conditions hold in central Au + Au collisions at several hundred MeV per nucleon, and probably hold up to α particles in non-central collisions at these energies. Overall, the EOS data lead to a conclusion that is generally compatible with the QMD calculations. Specifically, we find that the simple momentum-space power law describes the observed production of fragments up to αs in the participant zone over a remarkably wide range of conditions as long as fragments with low $p^{\perp}/A$ are excluded.

Assuming (a) we limit our consideration to data which satisfy the momentum-space power law, and (b) the quantity or quantities of interest can be defined in a coalescence-invariant form, and (c) these quantities are measured for all abundant fragment species, then the task of comparing transport models to experiment is greatly simplified and inferences from the comparisons should be more reliable. Directed flow is an obvious example of such a quantity of interest, and so our findings motivate a revisiting of flow comparisons, which should be based on coalescence-invariant experimental analyses (e.g., using $\langle Zp^x/A \rangle$ for protons through α particles, instead of the customary $\langle p^x/A \rangle$) and using the selection $p^{\perp}/A \geq 0.2$ GeV/c.

Our observation that adherence to the momentum-space power law deteriorates at lower $p^{\perp}/A$ cannot be readily interpreted in terms of dynamical correlations. Our comparison of QMD with the hybrid BUU-like calculation for 600A MeV Au + Au does not predict this effect. For example, we know that deviations from the power law will occur where proton and neutron spectra differ due to Coulomb effects. Single-particle-inclusive neutron[28] and proton[2] spectra have been published for the same system in the case of 0.8A GeV Ne + NaF; no differences within uncertainties are observed at large $p^{\perp}$, whereas at $p^{\perp}_{\rm neut} \sim 0.3$ GeV/c, proton spectra are shifted about 0.1 GeV/c. On the other hand, Coulomb distortion should be more prominent when comparing squared proton densities with deuteron densities than when comparing squared deuteron densities with α particle densities, and if anything, the observed deviations at low $p^{\perp}/A$ show the opposite tendency. Further study of fragment production at low $p^{\perp}/A$ is in progress.

4. Acknowledgements

This work is supported in part by the US Department of Energy under contract DE-AC03-76SF00098 and grants DE-FG02-89ER40531, DE-FG02-88ER40408, DE-FG02-88ER40412, DE-FG05-88ER40437, and by the US National Science Foundation under grant PHY-9123301.

5. References

1. H. H. Gutbrod, A. Sandoval, P. I. Johansen, A. M. Poskanzer, J. Gosset, W. G. Meyer, G. D. Westfall, and R. Stock, *Phys. Rev. Lett.* **37** (1976) 667;

J. Gosset, H. H. Gutbrod, W. G. Meyer, A. M. Poskanzer, A. Sandoval, R. Stock, and G. D. Westfall, *Phys. Rev. C* **16** (1977) 629.

2. M.-C. Lemaire, S. Nagamiya, S. Schnetzer, H. Steiner, and I. Tanihata, *Phys. Lett.* **85B** (1979) 38; S. Nagamiya, M.-C. Lemaire, E. Moeller, S. Schnetzer, G. Shapiro, H. Steiner, and I. Tanihata, *Phys. Rev. C* **24** (1981) 971.
3. S. Hayashi, Y. Miake, T. Nagae, S. Nagamiya, H. Hamagaki, O. Hashimoto, Y. Shida, I. Tanihata, K. Kimura, O. Yamakawa, T. Kobayashi, and X. X. Bai, *Phys. Rev. C* **38** (1988) 1229.
4. B. V. Jacak, D. Fox, and G. D. Westfall, *Phys. Rev. C* **31** (1985) 704.
5. N. Saito *et al., Phys. Rev. C* **49** (1994) 3211.
6. J. Barrette *et al., Phys. Rev. C* **50** (1994) 1077.
7. J. Aichelin and H. Stöcker, *Phys. Lett. B* **176** (1986) 14; J. Aichelin, *Phys. Rep.* **202** (1991) 233, and references therein.
8. G. Peilert, H. Stöcker, W. Greiner, A. Rosenhauer, A. Bohnet, and J. Aichelin, *Phys. Rev. C* **39** (1989) 1402.
9. P.-B. Gossiaux, D. Keane, S. Wang, and J. Aichelin, submitted to *Phys. Rev. C.*
10. H. W. Barz, J. P. Bondorf, R. Donangelo, R. Elmér, F. S. Hansen, B. Jakobsson, L. Karlsson, H. Nifenecker, H. Schulz, F. Schussler, K. Sneppen, and K. Söderström, *Nucl. Phys.* **A531** (1991) 453.
11. S. C. Jeong *et al., Phys. Rev. Lett.* **72** (1994) 3468.
12. W. C. Hsi *et al.*, preprint MSUNSCL-930, 1994.
13. M. A. Lisa *et al.*, preprint LBL-35504, 1994.
14. For reviews, see H. Stöcker and W. Greiner, *Phys. Rep.* **137** (1986) 277; G. F. Bertsch and S. Das Gupta, *Phys. Rep.* **160** (1988) 189.
15. G. Rai *et al., IEEE Trans. Nucl. Sci.* **37** (1990) 56.
16. E. Hjort *et al.*, in *"Advances in Nuclear Dynamics"*, (Proc. of 1993 Winter Workshop on Nuclear Dynamics, Key West, Florida), ed. B. Back, W. Bauer and J. Harris, (World Scientific, Singapore, 1993), p. 63.
17. M. L. Gilkes *et al., Phys. Rev. Lett.* **73** (1994) 1590.
18. H.-Å. Gustafsson *et al., Phys. Rev. Lett.* **52** (1984) 1590.
19. S. Wang *et al.*, preprint LBL-36077, 1994.
20. P. Danielewicz and G. Odyniec, *Phys. Lett.* **157B** (1985) 146.
21. M. B. Tsang *et al., Phys. Rev. Lett.* **57** (1986) 559.
22. K. G. R. Doss *et al., Phys. Rev. Lett.* **59** (1987) 2720.
23. C. A. Ogilvie *et al., Phys. Rev. C* **40** (1989) 2592.
24. J. P. Sullivan *et al., Phys. Lett. B* **249** (1990) 8.
25. G. D. Westfall *et al., Phys. Rev. Lett.* **71** (1993) 1986.

26. A. Kugler *et al.*, Proc. of *International Workshop XXII on Gross Properties of Nuclei and Nuclear Excitations*, ed. H. Feldmeier and W. Nörenberg, (GSI, Darmstadt, 1994), and *Phys. Lett. B* (in press).
27. H. Stöcker, A. A. Ogloblin, and W. Greiner, *Z. Phys.* **A303** (1981) 259; H. G. Baumgardt *et al., Z. Phys.* **A273** (1975) 359.
28. R. Madey *et al., Phys. Rev. Lett.* **55** (1985) 1453.